Nonlinear interaction of light with a Bose-Einstein condensate: Methods to generate sub-Poissonian light

I. Vadeiko*
School of Physics and Astronomy, University of St. Andrews, North Haugh, St. Andrews, KY16 9SS, Scotland

A. V. Prokhorov†
Vladimir State University, ul. Gorkogo 87, Vladimir, 600000 Russia

A. V. Rybin‡
Department of Physics, University of Jyväskylä, P.O. Box 35, FIN-40351 Jyväskylä, Finland

S. M. Arakelyan
Vladimir State University, ul. Gorkogo 87, Vladimir 600000 Russia
(Received 30 June 2004; published 6 July 2005)

We consider a Λ-type model of the Bose-Einstein condensate of sodium atoms interacting with the light. Coefficients of the Kerr nonlinearity in the condensate can achieve large and negative values, providing the possibility for effective control of group velocity and dispersion of the probe pulse. We find a regime when the observation of the "slow" and "fast" light propagating without absorption becomes achievable due to the strong nonlinearity. An effective two-level quantum model of the system is derived and studied. Our approach is based on a possibility of establishing a connection of the underlying algebra with the $su(2)$ algebra within the formalism of the polynomial algebras of excitations (PAE). We propose an efficient way for the generation of sub-Poissonian fields in the Bose-Einstein condensate at time-scales much shorter than the characteristic decay time in the system. We show that the quantum properties of the probe pulse can be controlled in BEC by the classical coupling field.

DOI: 10.1103/PhysRevA.72.013804 PACS number(s): 42.50.Ar, 42.50.Ct, 32.80.−t, 42.65.−k

I. INTRODUCTION

The problem of atom-field interaction represent one of the major areas in modern physics and quantum optics, in particular [1,2]. Special interest is directed to effects of propagation of light inside highly nonlinear atomic media, where a large nonlinearity is achieved through the appropriate choice of the form of the atom-field interaction [3,4]. Some early works [5,6] on the interaction of a resonance atomic system and laser field demonstrated the possibility of achieving a significant difference between phase and group velocity of the light pulses. Letokhov and Basov in their experiments have shown that while the front edge of the pulse generates the inversion in the system of two-level particles, which results in the sloping of the front edge of the pulse, the back-process of reemission of the absorbed energy gives rise to some steeping of the back edge of the pulse. Hence, the pulse shape deformation resulted in a significant delay of its registration on exit from the resonance media, and this phenomenon was observed experimentally. These observations motivated later intensive studies of the so-called "slow" and "fast" light.

An important step in the development of the theory was theoretical prediction [7] and experimental observation [8] of delayed or advanced registration of picosecond pulses propagating without pulse shape deformation inside a crystal. However, very high level of optical losses was limiting possibilities to observe the effects. Basically, there are several different ways to overcome the difficulty. The first idea exploits the shortening of the pulse duration to lengths, which would be much smaller than the relaxation times in the medium and this provides necessary conditions for generation of optical solitons [9]. Another approach is based on the features of the three-level Λ-scheme. In that case one of two laser beams is a strong coupling field developing a transparency window in the medium while the second probe field propagates through the resonant system without absorption and with unchanged pulse shape [10].

A picture of the energy levels for the Λ scheme for a single sodium atom is shown in Fig. 1. A classical beam with the central frequency ω_c couples the levels $|1\rangle$ and $|3\rangle$, and

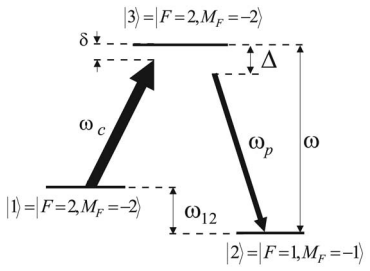

FIG. 1. The energy level Λ scheme of ^{23}Na atoms.

*Electronic address: iv3@st-andrews.ac.uk
†Electronic address: avprokhorov@front.ru
‡Electronic address: andrei.rybin@phys.jyu.fi

the probe pulse with central frequency ω_p couples $|3\rangle$ and $|2\rangle$ levels such that the three levels form a Λ-type configuration. If the intensities of the classical and probe fields are comparable and the relaxation rates of the levels $|1\rangle$ and $|2\rangle$ are negligible then a state of an atom can be considered as quantum superposition of two lower levels $|1\rangle$ and $|2\rangle$. This case corresponds to the effect of so-called coherent trapping of lower states [11,12]. Another type of dynamics may be realized if the intensity of the probe pulse is much smaller than the intensity of the classical field and the atoms initially populate the lower level $|2\rangle$. The regime is called electromagnetically induced transparency (EIT). In this paper we concentrate on the latter regime.

Systems in the EIT regime are extensively studied in the literature. Some interesting results are referred to: studies of the dispersion of atomic medium in the linear response regime [13], semiclassical estimates of the time delay of the probe field inside atomic cells in a thermal equilibrium [14], EIT in doped crystals [15], nonlinear optical parametric processes in resonant double-Λ system [16]. Wang and colleagues carried out important experimental measurements of the Kerr nonlinear index of refraction in a three-level Rb atomic Λ system using an optical ring cavity [17]. They found that the Kerr nonlinearity can reach very large and negative values.

One of the dominating problems in EIT was the spectrum broadening due to thermal effects. To overcome the difficulty, a highly coherent atomic Bose–Einstein condensate (BEC) is used [18,19]. Hau and co-workers calculated linear dispersive properties of the system and demonstrated a possibility to observe the "slow" light effect in the ultracold vapor of sodium atoms loaded into a magnetic trap at the temperature of transition to the condensed state [20]. Motivated by their results we consider EIT effects in the Bose–Einstein condensate of sodium atoms. Two hyperfine sublevels of sodium state $3^2S_{1/2}$ with $F=1$, $F=2$ are associated with levels $|2\rangle$ and $|1\rangle$ of the Λ scheme, correspondingly. An excited state $|3\rangle$ corresponds to the hyperfine sublevel of the term $3^2P_{3/2}$ with $F=2$ (see Fig. 1) [21]. The energy splitting between the levels $|1\rangle$ and $|2\rangle$ is denoted by $\omega_{12}/(2\pi)=1772$ MHz, the transition $|3\rangle\rightarrow|2\rangle$ corresponds to the optical frequency $\omega/(2\pi)=5.1\cdot10^{14}$ Hz ($\lambda=589$ nm) [22].

The condensate is assumed to be placed inside a confocal resonator. A strong coupling beam propagates along the optical axis of the resonator maintaining the transparency window in the condensate due to the transitions $|1\rangle\rightarrow|3\rangle$. According to the conventional EIT regime, the atoms mainly populate the lowest level $|2\rangle$. We assume that the resonator mode has an eigenfrequency ω_c. The coupling laser beam develops large polarization in the condensate, and this results in significant nonlinear susceptibility of the medium at the frequency ω_p. A probe pulse with the appropriately chosen polarization direction propagates transversely to the resonator optical axis. The interaction of the pulse with the condensate is highly nonlinear. In order to study a competition between linear and nonlinear processes connected to the transition $|3\rangle\rightarrow|2\rangle$ induced by the probe pulse, the linear and third order Kerr-like terms in the expansion of atomic susceptibility are considered. An effective control on the absorption of the probe pulse and its group velocity is realized through the "detuning" parameter Δ, which describes the difference of the probe field frequency from the resonance frequency.

In the following section we find conditions when the group velocity of the probe pulse becomes very small or very large. We also find a region where the absorption in the condensate is almost negligible. We interpret this phenomenon as the nonlinear compensation of optical losses. In the third section, the interaction between sodium BEC and the probe pulse is described by an effective quantum Hamiltonian. We explain how to reformulate the linear three level Λ scheme in terms of a nonlinear quantum model of two-level particles interacting with a quantized field and solve the problem. We apply the $su(2)$ polynomial deformation formalism in order to develop the perturbation theory. In the next section the perturbation theory is considered up to second order. In the last section we discuss some nonclassical effects in quantum statistics of the photons in the probe pulse described by the effective Hamiltonian. In conclusion we discuss the experimental relevance of our results.

II. NONLINEAR COMPENSATION IN SODIUM BEC

Applying the formalism of slowly varying field amplitudes [23] in the rotating wave approximation we write the Hamiltonian describing the interaction of three-level atoms with two laser fields in the following form [24]:

$$H^{\Lambda}=\omega_{12}|1\rangle\langle1|+\omega|3\rangle\langle3|,$$

$$-g_1|3\rangle\langle1|e^{-i\omega_c(t-z/c)}-g_1^*|1\rangle\langle3|e^{i\omega_c(t-z/c)},$$

$$-g_2|3\rangle\langle2|e^{-i\omega_p(t-z/c)}-g_2^*|2\rangle\langle3|e^{i\omega_p(t-z/c)}. \quad (1)$$

For simplicity, we assume $\hbar=1$. In Eq. (1) the coefficients $g_{1,2}$ determine single-photon Rabi frequencies and are defined as follows:

$$g_1=|\mu_{31}|A_c, \quad g_2=|\mu_{32}|A_p. \quad (2)$$

Here, μ_{ij} is the atomic dipole momentum, $A_{c(p)}$ are the slowly varying coupling and probe field amplitudes, correspondingly.

We denote the single-atom density matrix by $\rho=\Sigma_{\{i,j\}=1}^{3}\rho_{ij}|i\rangle\langle j|$. The time evolution of the density matrix is described by the Liouville equation of motion [25],

$$\frac{\partial\rho}{\partial t}=-i[H^{\Lambda},\rho]$$

$$-\gamma_{12}(|1\rangle\langle1|\rho-2|2\rangle\langle1|\rho|1\rangle\langle2|+\rho|1\rangle\langle1|),$$

$$-\gamma_{32}(|3\rangle\langle3|\rho-2|2\rangle\langle3|\rho|3\rangle\langle2|+\rho|3\rangle\langle3|),$$

$$-\gamma_{31}(|3\rangle\langle3|\rho-2|1\rangle\langle3|\rho|3\rangle\langle1|+\rho|3\rangle\langle3|). \quad (3a)$$

Here, the constants γ_{ij} determine the rates of spontaneous decay from the levels $|i\rangle$ to $|j\rangle$ in the Λ scheme. In general, to consider the space-time dynamics of the system of fields and

atoms interacting in the resonator we have to supplement Eq. (3) with the Maxwell equations, viz.,

$$\boldsymbol{\nabla} \times \boldsymbol{\nabla} \times \vec{\mathbf{E}} = -\frac{1}{c^2}\frac{\partial^2 \vec{\mathbf{E}}}{\partial t^2} - \frac{1}{\varepsilon_0 c^2}\frac{\partial^2 \vec{\mathbf{P}}}{\partial t^2}. \tag{3b}$$

Here, c is the velocity of light in the vacuum, $\vec{\mathbf{E}}$ is the amplitude of the field. The vector $\vec{\mathbf{P}}$ is the polarization of the condensate induced by the field.

In the adiabatic limit, when the variation of the Rabi frequency g_1 is very small [26] a self-consistent problem of Eqs. (3) and (3a) can be reduced to a less complicated one. In that case the system of equations can be solved separately for the medium and the fields. Through the averaging of the density matrix elements over the rapidly oscillating phase of the fields, we represent ρ in the form

$$\rho_{ii} = \bar{\rho}_{ii}, \quad \rho_{31} = \bar{\rho}_{31} e^{-i\omega_c(t-z/c)}, \quad \rho_{32} = \bar{\rho}_{32} e^{-i\omega_p(t-z/c)},$$

$$\rho_{12} = \bar{\rho}_{12} e^{-i(\omega_p-\omega_c)(t-z/c)}, \tag{4}$$

together with the relation $\bar{\rho}_{ij} = \bar{\rho}_{ji}^*$. An overbar in the matrix elements $\bar{\rho}$ denotes the averaged quantities. Substituting definitions Eq. (4) into Eq. (3), one obtains equations of motion for the matrix elements of $\bar{\rho}$, viz.,

$$\dot{\bar{\rho}}_{11} = -ig_1\bar{\rho}_{13} + ig_1^*\bar{\rho}_{31} - 2\gamma_{12}\bar{\rho}_{11} + 2\gamma_{31}\bar{\rho}_{33},$$

$$\dot{\bar{\rho}}_{22} = -ig_2\bar{\rho}_{23} + ig_2^*\bar{\rho}_{32} + 2\gamma_{12}\bar{\rho}_{11} + 2\gamma_{32}\bar{\rho}_{33},$$

$$\dot{\bar{\rho}}_{33} = ig_1\bar{\rho}_{13} - ig_1^*\bar{\rho}_{31} + ig_2\bar{\rho}_{23} - ig_2^*\bar{\rho}_{32} - 2(\gamma_{32}+\gamma_{31})\bar{\rho}_{33},$$

$$\dot{\bar{\rho}}_{21} = -i(\delta-\Delta)\bar{\rho}_{21} - ig_1\bar{\rho}_{23} + ig_2^*\bar{\rho}_{31} - \gamma_{12}\bar{\rho}_{21},$$

$$\dot{\bar{\rho}}_{31} = -i\delta\bar{\rho}_{31} + ig_1(\bar{\rho}_{11}-\bar{\rho}_{33}) + ig_2\bar{\rho}_{21} - (\gamma_{12}+\gamma_{32}+\gamma_{31})\bar{\rho}_{31},$$

$$\dot{\bar{\rho}}_{32} = -i\Delta\bar{\rho}_{32} + ig_2(\bar{\rho}_{22}-\bar{\rho}_{33}) + ig_1\bar{\rho}_{12} - (\gamma_{32}+\gamma_{31})\bar{\rho}_{32}. \tag{5}$$

Here, $\Delta = \omega - \omega_p$ and $\delta = \omega - \omega_{12} - \omega_c$.

We are interested in the nonlinear interaction of the BEC with a weak probe pulse in the dipole approximation. We study the explicit dependence of $\bar{\rho}_{32}$ on the Rabi frequency g_2 of the probe field in the limit $g_2 < \Delta$. In the vicinity of the resonance the condition is modified to the form $g_2 < \gamma_{32}$ [27]. The matrix element reads as

$$\bar{\rho}_{32} \approx \bar{\rho}_{32}^{(0)} + \bar{\rho}_{32}^{(1)} g_2 + \bar{\rho}_{32}^{(2)} |g_2|^2 + \bar{\rho}_{32}^{(3)} |g_2|^2 g_2. \tag{6}$$

The term $\bar{\rho}_{32}^{(0)}$ denotes initial spontaneous polarization, which vanishes for the sodium. The even-order terms like $\bar{\rho}_{32}^{(2)}$, $\bar{\rho}_{32}^{(4)}$ are finite only for asymmetric molecules, so we neglect these terms for sodium atoms as well. The coefficient $\bar{\rho}_{32}^{(1)}$ corresponds to the stationary solution of the system, Eq. (5), in the linear approximation and is responsible for the linear susceptibility of the medium. The nonlinear correction $\bar{\rho}_{32}^{(3)}$ determines resonant nonlinear atomic susceptibility denoted by $\chi^{(3)}$. Higher-order terms in the expansion, Eq. (6), are negligible in the regime of the weak probe field, which is the main focus of the present work.

We study the dynamics of $|2\rangle$ and $|3\rangle$ levels of sodium atoms interacting with the probe field. We characterize the transition $|2\rangle \rightarrow |3\rangle$ in terms of the effective coupling constant associated with the dipole matrix element $\bar{\rho}_{32}$. Assuming all the atoms to be initially in the state $|2\rangle$, i.e., $\bar{\rho}_{22}=1$, $\bar{\rho}_{11} = \bar{\rho}_{33} = 0$, we find from Eq. (5) [28],

$$\bar{\rho}_{32}^{(1)} = \frac{1}{\Gamma}, \quad \bar{\rho}_{32}^{(3)} = \frac{i}{\Gamma}\frac{\Gamma^* - \Gamma}{2|\Gamma|^2}\left(\frac{1}{2\gamma_{opt}} + \frac{1}{\gamma_{mag}}\right), \tag{7}$$

where

$$\Gamma = \Delta - i2\gamma_{opt} + \frac{|g_1|^2}{i\gamma_{mag} - \Delta}, \tag{8}$$

$$\gamma_{opt} = \frac{\gamma_{32}+\gamma_{31}}{2}, \quad \gamma_{mag} = \gamma_{12}. \tag{9}$$

A total polarization vector of the BEC coupled to the probe electromagnetic field is given in the form $\vec{\mathbf{P}} = \vec{\mathbf{P}}^{(l)} + \vec{\mathbf{P}}^{(nl)}$ [29]. Here $\vec{\mathbf{P}}^{(l)} = \epsilon_0 \hat{\chi}^{(1)} \cdot \vec{\mathbf{E}}$ describes the linear contribution, and

$$\vec{\mathbf{P}}^{(nl)} = \epsilon_0 (\hat{\chi}^{(2)} : \vec{\mathbf{E}}\vec{\mathbf{E}} + \hat{\chi}^{(3)} : \vec{\mathbf{E}}\vec{\mathbf{E}}\vec{\mathbf{E}} + \cdots) \tag{10}$$

is the nonlinear response on the external fields. The overcarets indicate tensorial objects. Using a well-known relation for the polarization induced in a resonance medium $\vec{\mathbf{P}} = (\mathcal{N}/V)\mu_{32}\bar{\rho}_{32}$ [2] and Eq. (7), we find the first- and third-order nonlinear susceptibilities of the Bose-Einstein condensate:

$$\chi^{(1)} = \frac{\mathcal{N}}{V}\frac{|\mu_{32}|^2}{\epsilon_0 \Gamma},$$

$$\chi^{(3)} = i\frac{2\mathcal{N}}{3V}\frac{|\mu_{32}|^4}{\epsilon_0}\frac{\Gamma^* - \Gamma}{\Gamma|\Gamma|^2}\left(\frac{1}{2\gamma_{opt}} + \frac{1}{\gamma_{mag}}\right). \tag{11}$$

Here $\mathcal{N}$ is a number of atoms in BEC, V is the volume, and $\mathcal{N}/V$ is the density of the condensate. Earlier, a similar form for the linear susceptibility $\chi^{(1)}$ of BEC in the EIT regime was obtained in the paper [20]. The nonlinear part $\chi^{(3)}$ of the Kerr type was studied in the regime of giant nonlinearities induced in a cyclic process of Λ-type interaction between optical fields and "hot" ^{87}Rb atoms in atomic cells inside an optical ring cavity [17].

The permittivity of the Bose gas corresponding to the probe field that includes the both linear and nonlinear terms reads [29] as

$$\epsilon_p = 1 + \chi^{(1)} + \frac{3}{4}\chi^{(3)}|A_p|^2. \tag{12}$$

Hence, using the relation $\epsilon_p = (n_p + i\eta_p c/2\omega_p)^2$ and Eq. (11), we find the refraction index n_p and the absorption coefficient η_p in the first order with respect to the intensity of the probe field,

$$n_p = n_p^{(0)} + n_p^{(2)}|A_p|^2, \quad n_p^{(0)} = 1 + \tfrac{1}{2}\,\mathrm{Re}(\chi^{(1)}),$$

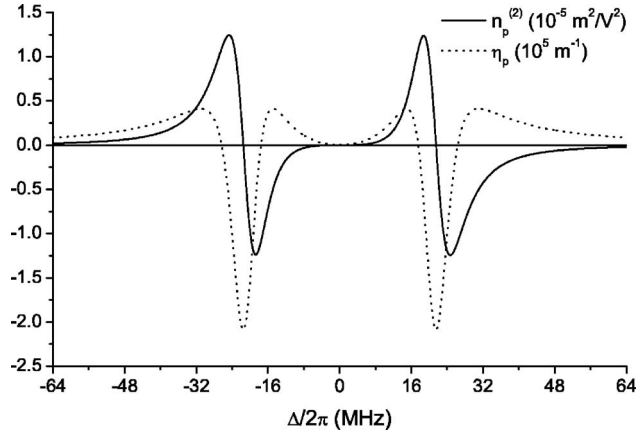

FIG. 2. The refraction index $n_p^{(2)}$ and the absorption coefficient η_p of ^{23}Na BEC as functions of the detuning Δ.

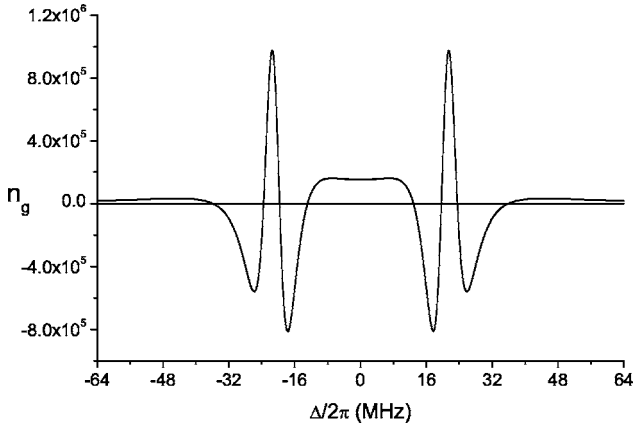

FIG. 3. The group refraction index n_g as a function of the detuning Δ.

$$n_p^{(2)} = \tfrac{3}{8}\,\mathrm{Re}(\chi^{(3)}); \tag{13}$$

$$\eta_p = \eta_p^{(0)} + \eta_p^{(2)}|A_p|^2, \quad \eta_p^{(0)} = \frac{\omega_p}{c}\,\mathrm{Im}(\chi^{(1)}),$$

$$\eta_p^{(2)} = \frac{3\omega_p}{4c}\,\mathrm{Im}(\chi^{(3)}). \tag{14}$$

In the present work the Bose–Einstein condensate is described by the Λ scheme near resonance. The density of sodium atoms in the condensate $\mathcal{N}/V = 3.3\cdot 10^{12}$ cm^{-3} is taken from [20] and the coupling field intensity $I_c = 55$ mW/cm^2. Taking the dipole matrix element $|\mu_{32}| = 22\times 10^{-30}$ C m from [30] and making use of the definition $A_c = \sqrt{2I_c/c\epsilon_0}$ [29] we calculate the coupling constant $g_1/(2\pi) = 21.4$ MHz. The probe pulse is assumed to have a time length of 1 μs, the laser waist inside the BEC is $d = 3.7$ μm. The intensity of the probe pulse $I_p = 80$ μW/cm^2 corresponds to 25 photons on average.

Due to atomic coherence in the BEC, in the absence of the Doppler broadening the decay rates γ_{31} and γ_{32} of the level $|3\rangle$ can be estimated by the widths of spontaneous transitions from the upper levels of sodium atoms. Taken from the paper [30] the lifetime for the upper level is $T_{rel} = 16.3$ ns; therefore we assume $\gamma_{32}/2\pi = \gamma_{31}/2\pi = 5$ MHz. The decay rates of transitions between the hyperfine levels $|1\rangle$ and $|2\rangle$ is $\gamma_{12}/(2\pi) = 38$ KHz, Ref. [2].

In Fig. 2 we plot a typical frequency dependence of the nonlinear optical refraction index and absorption coefficient as functions of detuning Δ. Giant nonlinear refraction index formed in the condensate with appropriately chosen detuning of the probe pulse is used in this paper to demonstrate the possibility of generating sub-Poissonian statistics of photons on very short time scales. It is also worth noticing that the realization of negative $n_p^{(2)}$ is similar to the effects observed in [17], and can have some important physical applications.

On the other hand, the alternation of regions with positive and negative absorption coefficients corresponds to the regimes of effective nonlinear attenuation or amplification of the probe field intensity in the BEC. In both cases, the energy is transferred between the coupling field and the probe pulse. The case of zero absorption $\eta_p = 0$ can be characterized as a nonlinear EIT. Notice that the regime of complete absence of optical losses in the system falls in the region of very large values of $n_p^{(2)}$. This opens even more broad perspectives to generate nonclassical light in the system. In general, varying the intensity of the coupling and probe light, and the detuning Δ, we can control the parameter Γ in Eq. (11) and change the relative impact of the linear and nonlinear effects on the probe pulse in the condensate.

To understand the effect of "slow" light in the system we study a frequency dependence of some characteristics of the probe pulse envelope. In Fig. 3 we plotted the group refraction index $n_g = n_p + \omega_p(dn_p/d\omega_p)$ [31]. A point $\Delta = 0$ of the exact resonance corresponds to the EIT regime [10] characterized by low losses and large n_g. Under chosen resonance conditions, the group velocity $v_g = c/n_g$ is at 2000 m/s while the losses are $\eta_p = 242$ m^{-1}. So, the regime corresponds to the effect of "slow" light in much the same way as it was demonstrated in the linear limit of the theory of EIT [14]. An interesting point in Fig. 3 is a zero of the group refraction index n_g that indicates an uncertainty of the group velocity v_g of the probe pulse. The uncertainty reflects the possibility of observing superluminal velocities. This effect, together with the negative group refraction index, is explained in the literature [7,32] by the presence of plane waves of different frequencies, which appear in the medium long before the pulse peak enters into it. When the group velocity is negative ($n_g < 0$) the pulse generates two antipropagating pulses in the BEC. One of them propagates backward (negative velocity) and prevents the peak from traveling forward in the medium.

In the following sections we concentrate on some effects in dynamics of the weak probe pulse. These effects are induced in the system of highly correlated three-level particles by relatively strong classical coupling field. We show how the latter can control some quantum properties of the probe pulse.

III. THE EFFECTIVE TWO-LEVEL QUANTUM MODEL

We are interested in quantum properties of the probe field and therefore define the field in terms of creation and anni-

hilation operators $a^\dagger, a$. The dynamics of the probe field is defined by only two levels, i.e. $|2\rangle$ and $|3\rangle$, and we work in the EIT limit, when the largest part of the atoms is concentrated on the lower level $|2\rangle$. We assume that the classical field is strong and describe its influence in terms of the effective coupling constant for the probe field. The effective two-level Hamiltonian in dipole and rotating wave approximations reads as

$$H = \omega_p(a^\dagger a + S_3 + \mathcal{N}/2) + \Delta S_3 + k_1(aS_+ + a^\dagger S_-) + k_2(a^\dagger a a^\dagger S_- + a a^\dagger a S_+). \quad (15)$$

The operators $S_\pm$, S_3 describe total dipole momentum corresponding to the transitions $|3\rangle \leftrightarrow |2\rangle$ for the atoms in BEC. The first and the second terms give the free energy of the probe field and atoms. The third term describes linear contribution into the interaction between the field and two-level particles in dipole approximation. It has the typical form of the so-called Tavis-Cummings [33] or Dicke model [34]. The last term in Eq. (15) describes nonlinear processes existing due to the presence of a strong classical coupling field. This term depends on the intensity of the probe pulse. The both coupling constants $k_{1,2}$ are defined below.

An interaction between the BEC and the probe field is determined by the effective matrix element of atomic dipole momentum between $|2\rangle$ and $|3\rangle$ levels. Due to induced nonlinearity, the matrix element depends on the intensity of the probe field described by the operator $a^\dagger a$ and on the intensity of the coupling field given by a c-number parameter. We define the overall coupling constant in the dipole approximation as follows:

$$k_0 \frac{\bar{\rho}_{32}(g_1, \Delta, g_2)}{\bar{\rho}^{(1)}_{32}(g_1 = 0, \Delta) g_2}, \quad (16)$$

where $\bar{\rho}_{32}$ is given in Eq. (6), and $k_0 = \mu_{32}\sqrt{\omega/2\hbar\varepsilon_0 V}$ is the single-photon Rabi frequency in the Dicke model [35]. The form factor in Eq. (16) satisfies the condition that at zero coupling field it approaches unity. This behavior of the form factor results from the fact that when $g_1 \approx 0$ the induced nonlinearity for the probe field should vanish.

From the definition, Eq. (16), and the expansion of $\bar{\rho}_{32}$ in Eqs. (6) and (7), we find the coupling constants k_1 and k_2,

$$k_1 = k_0 L_l, \quad k_2 = k_0^3 L_{nl}, \quad (17)$$

The parameters $L_{l(nl)}$ denote linear and nonlinear form factors (compare with [36]), correspondingly

$$L_l = \frac{\bar{\rho}^{(1)}_{32}(g_1, \Delta)}{\bar{\rho}^{(1)}_{32}(g_1 = 0, \Delta)}, \quad L_{nl} = \frac{\bar{\rho}^{(3)}_{32}(g_1, \Delta)}{\bar{\rho}^{(1)}_{32}(g_1 = 0, \Delta)}. \quad (18)$$

As far as the phase of the probe field is arbitrary we can choose it in such a way that k_1 would be a real number with $\tilde{L}_l = |L_l|$. In that case the nonlinear coupling constant would be defined with $\tilde{L}_{nl} = e^{-i \arg(L_l)} L_{nl}$.

According to this formulation we are able to dynamically control the rates of the transitions induced by the quantum probe field A_p with help of the classical field A_c. Changing the latter, one can reach qualitatively different regimes of the quantum dynamics described by the effective Hamiltonian equation (15).

The effective Hamiltonian can be expressed in terms of fifth-order polynomial algebra of excitations (PAE) [37]. The generators M_0, $M_\pm$ of the algebra are realized as follows:

$$M_0 = \frac{a^\dagger a - S_3}{2}, \quad M_+ = \left(1 + \frac{k_2}{k_1} a^\dagger a\right) a^\dagger S, \quad (19)$$

and $M_- = (M_+)^\dagger$. These generators M_0, $M_\pm$ satisfy basic commutation relation for any PAE,

$$[M_0, M_\pm] = \pm M_\pm, \quad (20)$$

and commute with the operators

$$M = a^\dagger a + S_3 + r, \quad S^2 = S_3^2 + \frac{1}{2}(S_+ S_- + S_- S_+). \quad (21)$$

Hereafter we use the same notation M both for the Casimir operator and its eigenvalue, if no confusion arises. It is known that the eigenvalues M, $r(r+1)$ of the operators in Eq. (21) parametrize the PAE in question. We thus denote this PAE by $\mathbb{M}_{M,r}$. The structure polynomial of $\mathbb{M}_{M,r}$ can be expressed in the form

$$p_5(M_0) = M_+ M_- = a^\dagger a \left(1 + \frac{k_2}{k_1} a^\dagger a\right)^2 (S^2 - S_3^2 - S_3) = -\left(M_0 + \frac{M-r}{2}\right)\left(1 + \frac{k_2}{k_1} M_0 + \frac{k_2}{k_1}\frac{M-r}{2}\right)^2 \left(M_0 - \frac{M-3r}{2}\right) \times \left(M_0 - \frac{M+r+2}{2}\right). \quad (22)$$

The parameters of this structure polynomial are

$$c_0 = -\left(\frac{k_2}{k_1}\right)^2, \quad q_0 = -\left(\frac{k_1}{k_2} + \frac{M-r}{2}\right), \quad q_1 = -\frac{M-r}{2}$$

$$q_2 = \frac{M-r}{2} - r, \quad q_3 = \frac{M-r}{2} + r + 1. \quad (23)$$

Notice that q_0 is a degenerate root of order 2.

Following standard procedure [37], we describe a physically interesting finite-dimensional irreducible representation (irrep) of $\mathbb{M}_{M,r}$. In our model the parameter r has the meaning of a collective Dicke index [34] (an analog of the orbital momentum) of the system of $\mathcal{N}$ two-level particles. This index runs from $\varepsilon(\mathcal{N}) = [1 - (-1)^{\mathcal{N}}]/4$ to $\mathcal{N}/2$ with unit steps, while M can be any natural number including zero, as follows from the definition in Eq. (21). A physically interesting irrep of $\mathbb{M}_{M,r}$ is characterized by such two roots of the structure polynomial that the polynomial takes positive values between them. The roots $q_{1,2,3}$ do not depend on the ratio k_1/k_2 and are ordered according to the relation between M and r. For $M \geqslant 2r$, $q_1 < q_2 \leqslant q_3$, and for $M < 2r$, $q_2 < q_1 < q_3$. Since the root q_0 is of order 2, its position on the real axis does not influence the region where the structure polynomial is non-negative. Hence, if $M > 2r$, the irrep is called a *remote* zone and $p_5(x)$ is non-negative in the interval

$[q_2, q_3]$, whereas if $M < 2r$ the irrep is called a *nearby* zone and $p_5(x)$ is non-negative in the interval $[q_1, q_3]$. Notice that the region $M \gg 2r$ is usually called the strong-field limit and the region $M \ll 2r$ is usually called the weak-field limit. The case $M = 2r$ is of a special kind and the corresponding irrep is called the boundary zone.

Depending on the value of the ratio k_1/k_2 we have two different situations. If q_0 does not belong to the interval where $p_5(x) \geqslant 0$, the polynomial is approximated by the parabolic function relatively well. The parabolic approximation is described in our previous paper [37]. In case q_0 belongs to the interval of positiveness of $p_5(x)$, we must introduce some changes to the approach. But for the physical system considered here the ratio takes large negative values and the total number of excitations M can be assumed to be smaller than the ratio, i.e. $M < |k_1/k_2| - 1$. Therefore, q_0 is always larger than q_3, and we can use the algebraic approach developed for a conventional Tavis-Cummings model.

In the physical situation studied here, the remote and nearby zones are bounded by nondegenerate roots of $p_5(x)$ and the corresponding physical irrep of the fifth-order PAE $\mathbb{M}_{M,r}$ is isomorphic to the physical irrep of second-order PAE, denoted in the paper as $\mathbb{S}_{\tilde{r}}$. Here we use $\tilde{r}$ to distinguish it from collective Dicke index r describing the two-level system. We solve the eigenvalue problem of the Hamiltonian, Eq. (15), in terms of simpler algebra $\mathbb{S}_{\tilde{r}}$ using the isomorphism between the algebras. The idea is straightforward. The generators $M_{\pm}$, M_0 are realized in terms of the generators $\tilde{S}_{\pm}$, $\tilde{S}_3$ of $\mathbb{S}_{\tilde{r}}$ according to the isomorphism and substituted into the Hamiltonian. The interaction part is expanded into perturbation series of power of the operator $\tilde{S}_3$ and the series are diagonalized by consecutive unitary transformations. More accurate, however, more technically involved, approximations of the effective Hamiltonian equation, Eq. (15), are described in Appendix A.

To begin with we consider the transformation of $\mathbb{M}_{M,r}$ to $\mathbb{S}_{\tilde{r}}$ for the case of remote zones. The dimension of a remote zone is $2r+1$. Hence, the algebra $\mathbb{S}_{\tilde{r}}$ is characterized by $\tilde{r} = r$. The finite-dimensional irrep of $\mathbb{S}_{\tilde{r}}$ is isomorphic to the corresponding irreducible representation of $su(2)$ algebra. The corresponding transformation from the generators of $\mathbb{M}_{M,r}$ to the generators of $\mathbb{S}_{\tilde{r}}$ is defined as follows (see [37])

$$M_0 = \frac{M-r}{2} - \tilde{S}_3,$$

$$M_+ = \tilde{S}_- \sqrt{M - r + 1 - \tilde{S}_3}\left(1 + \frac{k_2}{k_1}(M - r + 1 - \tilde{S}_3)\right). \quad (24)$$

Spectrum $\{\tilde{m}\}$ of the operator $\tilde{S}_3$ belongs to the interval $[-r, r]$ so the argument of the square root function in Eq. (25) has a positive-valued spectrum in the remote zones ($M > 2r$). Expanding the root function with respect to $\left(\tilde{S}_3 - \frac{1}{2}\right)$ we obtain the perturbation series with smallness parameter $\alpha = 1/(M - r + \frac{1}{2})$.

It is worth noticing the connection between new operators $\tilde{S}_{\pm}$, $\tilde{S}_3$ and the physical operators of the model. From Eqs. (19), (21), and (25) it follows that in remote zones,

$$\tilde{S}_3 = S_3, \quad \tilde{S}_+ = \frac{1}{\sqrt{a^\dagger a + 1}} a S_+, \quad \tilde{S}_- = (\tilde{S}_+)^\dagger. \quad (25)$$

Notice that the subspaces corresponding to the remote zones do not contain the vacuum state of the field. It is also worth mentioning that the matrix representation of the operator $(1/\sqrt{a^\dagger a + 1})a$ is $\delta_{n,n+1}$ for any remote zone. This operator has been considered before in terms of phase operator [38–40].

We turn now to the nearby zones $M < 2r$. Notice that the dimension of nearby zones is $q_3 - q_1 = M + 1$, and therefore $\tilde{r} = M/2$. Hence, we obtain the following realization:

$$M_0 = r/2 - \tilde{S}_3, \quad M_- = (M_+)^\dagger,$$

$$M_+ = \tilde{S}_- \sqrt{\frac{4r - M}{2} + 1 - \tilde{S}_3}\left(1 + \frac{k_2}{k_1}\left(\frac{M}{2} + 1 - \tilde{S}_3\right)\right). \quad (26)$$

Since all the eigenvalues of the operator $\tilde{S}_3$ belong to the interval $[-\tilde{r}, \tilde{r}]$, the argument of the square root function does not have zero eigenvalues in the nearby zones. The realization of $\mathbb{S}_{\tilde{r}}$ through spin and boson variables is then given by

$$\tilde{S}_3 = \frac{M}{2} - a^\dagger a, \quad \tilde{S}_+ = \frac{1}{\sqrt{r + 1 - S_3}} S_+ a. \quad (27)$$

Notice that the nearby zones do not contain the eigenvector $|r, r\rangle$ of S_3.

IV. DIAGONALIZATION PROCEDURE

We start with the representation of the Hamiltonian equation, Eq. (15), in the form of series with respect to the operator $\alpha\left(\tilde{S}_3 - \frac{1}{2}\right)$, where the constant α is a smallness parameter specified below. As we already mentioned, to construct the series we expand the square root function in the realizations, Eq. (25) and Eq. (26). The expansion parameter depends on the zone under consideration and has the form

$$\alpha \equiv \begin{cases} \dfrac{1}{M - r + \dfrac{1}{2}}, & M \geqslant 2r \\ \dfrac{2}{4r - M + 1}, & M < 2r \end{cases}. \quad (28)$$

An accuracy necessary to observe all the interesting effects described in the paper is provided by the first three terms in the expansion of the effective Hamiltonian equation, Eq. (15). Up to the second order with respect to the smallness parameter α it reads as

$$H \approx \omega_p\left(M+\frac{\mathcal{N}}{2}-r\right)+\Delta(\tilde{S}_3+\tilde{r}-r) + k\left[\begin{array}{c}\dfrac{\tilde{S}_+ + \tilde{S}_-}{2} - \dfrac{\beta_1}{4}\left(\left(\tilde{S}_3-\dfrac{1}{2}\right)\tilde{S}_+ + \tilde{S}_-\left(\tilde{S}_3-\dfrac{1}{2}\right)\right) \\ -\dfrac{\beta_2}{2}\left(\left(\tilde{S}_3-\dfrac{1}{2}\right)^2\tilde{S}_+ + \tilde{S}_-\left(\tilde{S}_3-\dfrac{1}{2}\right)^2\right)\end{array}\right]. \tag{29}$$

Here we used a simple relation $S_3=\tilde{S}_3+\tilde{r}-r$. To prove it one should utilize the definition of $\tilde{r}$ given in the previous section in the remote or nearby zones, and the relations Eqs. (25) and (27). The parameters in Eq. (29) are defined as follows:

$$\gamma=\begin{cases}1+\dfrac{k_2}{k_1}\left(M-r+\dfrac{1}{2}\right), & M \geqslant 2r \\ 1+\dfrac{k_2}{k_1}\dfrac{M+1}{2}, & M<2r\end{cases} \tag{30}$$

$$k=k_1\gamma\frac{2}{\sqrt{\alpha}},$$

$$\beta_1=\alpha\left(1+\frac{k_2}{k_1}\frac{2}{\gamma\alpha}\right), \quad \beta_2=\alpha^2\left(\frac{1}{8}-\frac{k_2}{k_1}\frac{1}{2\gamma\alpha}\right). \tag{31}$$

Considering the irreducible representations of the fifth-order algebra $\mathbb{M}_{M,r}$ above, we noticed a limitation on the value M necessary for the algebraic approach to the Tavis-Cummings model to be applicable. A relatively accurate approximation of the structure polynomial $p_5(x)$ by the parabolic polynomial of $\mathbb{S}_{\tilde{r}}$ in the interval between the two roots where $p_5(x)$ takes positive values is achievable if q_0 does not belong to the interval. Now we are able to define the limitation of the algebraic approach more rigorously. We find from Eqs. (30) and (31) that $\gamma \sim O(1)$ and $\beta_n \sim \alpha^n$ if

$$M+1<\left|\frac{k_1}{k_2}\right|. \tag{32}$$

The Hamiltonian, Eq. (29), can be rearranged into the following form:

$$H^{(2)}=C_0+\Delta\tilde{S}_3+k\left[\tilde{S}_x-\frac{\beta_1}{4}(\tilde{S}_3\tilde{S}_x+\tilde{S}_x\tilde{S}_3) - \beta_2\left(\tilde{S}_3\tilde{S}_x\tilde{S}_3+\frac{1}{4}\tilde{S}_x\right)\right], \tag{33}$$

where $\tilde{S}_x=(\tilde{S}_+ + \tilde{S}_-)/2$ according to the $su(2)$ algebra notations, and $C_0=\omega_p(M+\mathcal{N}/2-r)+\Delta(\tilde{r}-r)$ is a constant in each irreducible representation because M is the Casimir operator.

The first three terms in Eq. (33) are linear with respect to the generators of $\mathbb{S}_{\tilde{r}}$ and can be diagonalized by well-known $su(2)$ unitary transformation $U_0=e^{(i\psi_0\tilde{S}_y)}$ corresponding to rotation of the quasispin vector $(\tilde{S}_x,\tilde{S}_y,\tilde{S}_3)$ about the y axis, where $\tilde{S}_y=(\tilde{S}_+-S_-)/2i$. The angle ψ_0 is found from the relations

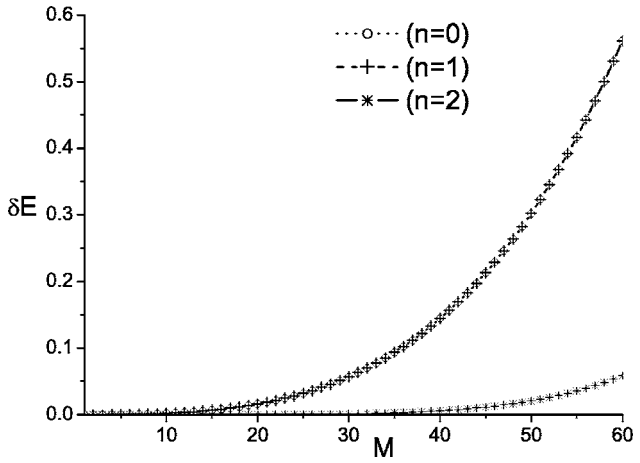

FIG. 4. Relative error, $\delta E(M)=\max((E(M)-E^{(n)}(M))/\Delta E(M))$, for three different orders of accuracy ($n=0,1,2$). Here, $E(M)$ is the exact spectrum of the Hamiltonian, Eq. (15), calculated numerically in the irrep specified by given M and r values, $\Delta E(M)$ is an average splitting between the spectrum levels, and $E^{(n)}(M)$ is the spectrum calculated by Eq. (35) in nth order with respect to α. For the condensate, we choose $\mathcal{N}=1000$; hence $r=\mathcal{N}/2$. For the field, the parameters $\Delta/\omega_p=2.4E-8$, $k_1/\omega_p=3.04E-7$, $k_2/\omega_p=-3.01E-9$ are taken according to the consideration in the previous section.

$$\cos(\psi_0)=\frac{\Delta}{\Omega_R}, \quad \sin(\psi_0)=\frac{k}{\Omega_R}, \quad \Omega_R=\sqrt{\Delta^2+k^2}, \tag{34}$$

where we introduced a notion of nonlinear quantum Rabi frequency Ω_R. Hence, after the transformation $U_0H^{(2)}U_0^{-1}$ a zeroth-order contribution into Eq. (33) with respect to α reads as $(C_0+\Omega_R\tilde{S}_3)$, which justifies the name for the constant Ω_R. It describes the frequency of rotation of the quasispin $\tilde{r}$ of the atom-field quantum system.

Applying two additional unitary transformations U_1, U_2 discussed in Appendix B, we diagonalize the Hamiltonian up to the second order with respect to α. The diagonalized operator takes the form

$$\begin{aligned}H^{(2)}_{diag}(\tilde{S}_3) &= (U_2U_1U_0)H^{(2)}(U_2U_1U_0)^{-1}=C_0+\Omega_R\tilde{S}_3 \\ &-\frac{\beta_1}{4}\frac{k^2\Delta}{\Omega_R^2}(3\tilde{S}_3^2-\tilde{r}(\tilde{r}+1)) \\ &+\left(\frac{\beta_1}{4}\right)^2\frac{k^2}{\Omega_R}\tilde{S}_3\left[\frac{4\Delta^4-9\Delta^2k^2+4k^4}{\Omega_R^4}\tilde{S}_3^2\right. \\ &\left.-\frac{2\Delta^4-5\Delta^2k^2+2k^4}{\Omega_R^4}\tilde{r}(\tilde{r}+1)+\frac{1}{2}\frac{\Delta^4+\Delta^2k^2+k^4}{\Omega_R^4}\right] \\ &-\frac{\beta_2}{2}\frac{k^2}{\Omega_R}\tilde{S}_3\left[\frac{4\Delta^2-k^2}{\Omega_R^2}\tilde{S}_3^2-\frac{2\Delta^2-k^2}{\Omega_R^2}\tilde{r}(\tilde{r}+1)\right. \\ &\left.+\frac{1}{2}\frac{\Delta^2-k^2}{\Omega_R^2}\right]+o(\alpha^2).\end{aligned} \tag{35}$$

In Fig. 4 we compare the second-order solution, Eq. (35), with the exact numerical diagonalization of H, Eq. (15), and find that the approximation is very accurate and does not significantly depend on the number $\mathcal{N}$ of the particles in the

condensate. Basically, the higher is the ratio $|M-2r|/2r$, the better the analytical solution, Eq. (35), becomes. The first-order correction to the spectrum [of order β_1 in Eq. (35)] is proportional to the detuning Δ and vanishes at the point of exact resonance. Therefore, the relative error decreases significantly only if the second order correction is taken into account. One can understand from Fig. 4 that at the points where zeroth- and first-order errors increase to 50% our second-order correction provides accuracy even higher than 95%. The plot shows the typical behavior of the second-order solution in the nearby zones. According to the condition, Eq. (32), the approximation diverges when we approach too close to the point $|k_1/k_2|-1=100$. Therefore, we restrict our initial state of the system to the maximum of 60 excitations. It is justified in the next section from the physical point of view.

V. SUB-POISSONIAN DISTRIBUTION IN PHOTON STATISTICS

To study photon statistics we have to construct the time evolution of corresponding field operators. It is well known that the simplest characteristic of the sub-Poissonian nature of the photon distribution is the Fano-Mandel parameter $Q(t)$, defined as follows:

$$Q(t)=\frac{\langle (a^{\dagger}a)^2\rangle-\langle a^{\dagger}a\rangle^2}{\langle a^{\dagger}a\rangle}-1. \tag{36}$$

Our unitary transformation approach allows us to represent the averages of field operators in Eq. (36) in the following convenient form:

$$\langle A(t)\rangle=\langle\Phi_0|e^{iHt}Ae^{-iHt}|\Phi_0\rangle \approx\langle\Phi_0|U_0^{-1}(e^{iH_{diag}^{(2)}t}U_0AU_0^{-1}e^{-iH_{diag}^{(2)}t})U_0|\Phi_0\rangle, \tag{37}$$

where $|\Phi_0\rangle$ is an initial state of the atom-field system and A is an arbitrary operator. In Eq. (37) we include only zeroth-order terms with respect to α, i.e., $U_{1,2}\to 1$. Notice that, because the time intervals of interest may be relatively large, in the diagonalized Hamiltonian $H_{diag}^{(2)}(\tilde{S}_3)$ the terms up to second-order terms are included. Applying the relation $a^{\dagger}a=M-\tilde{S}_3-\tilde{r}$, it is straightforward to find the time dependence of $A=a^{\dagger}a$ from Eq. (37). The result reads as

$$e^{iH_{diag}^{(2)}t}U_0a^{\dagger}aU_0^{-1}e^{-iH_{diag}^{(2)}t}=M-\tilde{r}-\frac{\Delta}{\Omega_R}\tilde{S}_3 +\frac{k}{2\Omega_R}(\tilde{S}_+e^{it[H_{diag}^{(2)}(\tilde{S}_3+1)-H_{diag}^{(2)}(\tilde{S}_3)]} +\text{H.c.}). \tag{38}$$

Taking the square of the expression, Eq. (38), one easily finds corresponding formula for $A=(a^{\dagger}a)^2$. To calculate the parameter $Q(t)$ we have to average these operators over a unitary transformed initial state, i.e., over $U_0|\Phi_0\rangle$. The transformation U_0 is studied in detail in the theory of the $su(2)$ algebra. Should we be able to represent the initial atom-field state $|\Phi_0\rangle$ in the basis of eigenstates $|\tilde{m},\tilde{r}\rangle$ of the operator $\tilde{S}_3$, then each of the vectors $|\tilde{m},\tilde{r}\rangle_{dr}\equiv U_0|\tilde{m},\tilde{r}\rangle=\Sigma_{\tilde{m}'=-\tilde{r}}^{\tilde{r}}B_{\tilde{m},\tilde{m}'}|\tilde{m}',\tilde{r}\rangle$ is the well-known coherent state of the $su(2)$ algebra. In the theory of atom-field interaction the states $|\tilde{m},\tilde{r}\rangle_{dr}$ are usually called generalized atom-field dressed states.

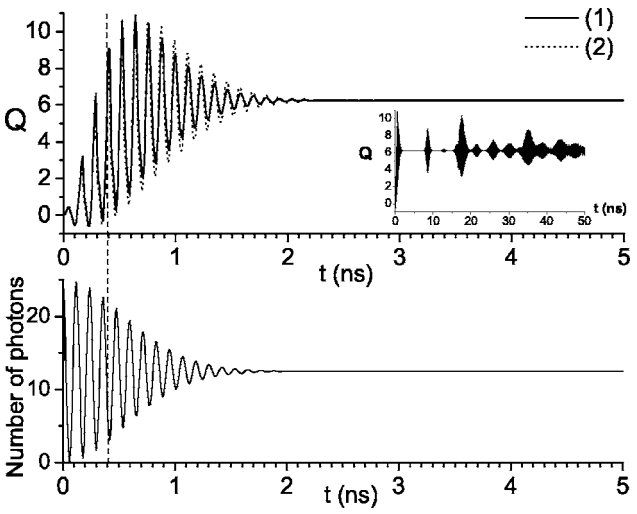

FIG. 5. The Fano-Mandel parameter $Q(t)$ and the average number of photons for initially unexcited sodium BEC and a coherent probe field with $n_0=25$ average number of photons. All the parameters are the same as in Fig. 4. The solid line (1) on the plot of $Q(t)$ is calculated in second order of α according to Eq. (37). The dotted line (2) is calculated by Eqs. (40) and (41).

In this paper we choose experimentally plausible initial state of the sodium BEC. The probe field is prepared in a coherent state with average number of photons $n_0=25$. The atoms are prepared in completely symmetrized unexcited eigenstate of the operator S_3, i.e., $|m_0,r=\mathcal{N}/2\rangle$, with zero number of excitations $(m_0+\mathcal{N}/2=0)$. Hence,

$$|\Phi_0\rangle=\left|-\frac{\mathcal{N}}{2},\frac{\mathcal{N}}{2}\right\rangle\otimes\sum_{n=0}^{\infty}\sqrt{e^{-n_0}\frac{n_0^n}{n!}}|n\rangle =\sum_{n=0}^{\infty}\sqrt{e^{-n_0}\frac{n_0^n}{n!}}\left|\tilde{m}=-\frac{n}{2},\tilde{r}=\frac{n}{2}\right\rangle. \tag{39}$$

The last equality follows from the relations Eqs. (21) and (27), because for completely unexcited atoms the total number of excitations M is equal to the number of photons n. Having represented the initial state in the basis of the eigenvectors of the operator $\tilde{S}_3$ we can immediately calculate the Fano-Mandel parameter Q. Below in Fig. 5 we plot the evolution of $Q(t)$ and the average number of photons for such initial state. Regions where the parameter $Q(t)$ takes negative values correspond to sub-Poissonian distribution in statistics of photons in the probe pulse. First, we notice that the minimum of $Q(t)$ is reached after the second Rabi oscillation, which is described by corresponding Rabi frequency Ω_R given in Eq. (34). The frequency depends on the number of excitations M. Being calculated for the average initial number of excitations $M=n_0$ it gives the period of Rabi oscillation $T_R=2\pi/\Omega_R=0.12$ ns, which is confirmed by Fig. 5 (see

the dynamics of the average number of photons). The time interval where the probe pulse shows maximum squeezing in fluctuations of the number of photons, is approximately 0.5 ns that is much smaller than the relaxation times in BEC (T_{rel}=16.3 ns). This time scale satisfies the adiabatic condition imposed above. The dispersion of photons in the initial coherent state is equal to the average number of photons, i.e. to n_0=25. It means that the probability to find more than $2n_0$=50 photons is negligible and the restriction from above on the number of excitations $M < |k_1/k_2| \approx 100$ in the system is fulfilled as well.

We can notice in Fig. 5 that the maximum squeezing is relatively large, $Q \approx -0.6$. It is observed after two cycles of almost complete absorption and reemission of the photons by sodium BEC that is represented by the plot of the average number of photons in the probe pulse in Fig. 5. The quantum effect is provided by the correlation in the atomic system, which is transferred to the field after two complete Rabi cycles of the collective atom-field quasispin $\tilde{S}_3$.

The small subplot of the parameter $Q(t)$ in Fig. 5 at a large time scale shows that the effect has very short lifetime and only appears in the beginning of the evolution. The regular collapses and revivals are observed due to the interference between Rabi oscillations with different frequencies. The effect is wellknown in the one-atom case, and the collapse and revival times were estimated in the single-particle model [41]. We will show now that due to the nonlinear interaction between sodium atoms and the probe pulse the maximum squeezing of photon statistics is achieved much faster than in the regular Dicke model. This fact plays a crucial role in taking into account different mechanisms of the decoherence and relaxation in the system. For instance, the adiabatic approach developed in the paper will break down if the nonlinear terms are not included in the Hamiltonian.

Since we are interested in a short time-scale dynamics, we can neglect higher-order corrections to the spectrum of the Hamiltonian, Eq. (35), keeping only zeroth order terms in Eq. (37). Then, we find

$$\langle a^\dagger a(t)\rangle = \langle \Phi_0|(M-\tilde{r})(1-\cos(\Omega_R t))\sin(\psi_0)^2|\Phi_0\rangle + \langle \Phi_0|a^\dagger a(\cos(\psi_0)^2 + \sin(\psi_0)^2\cos(\Omega_R t))|\Phi_0\rangle, \tag{40}$$

$$\langle a^\dagger a(t)^2\rangle = \langle \Phi_0|(a^\dagger a)^2\Big[\cos(\psi_0)^4 + \cos(\psi_0)^2\sin(\psi_0)^2(3\cos(\Omega_R t)-1) + \frac{1}{4}\sin(\psi_0)^4(1+3\cos(\Omega_R t))\Big]|\Phi_0\rangle + \langle \Phi_0|a^\dagger a\Big[(M-\tilde{r})\sin(\psi_0)^2\sin\Big(\frac{\Omega_R}{2}t\Big)^2(5+3\cos(2\psi_0) + 6\sin(\psi_0)^2\cos(\Omega_R t))\Big]|\Phi_0\rangle,$$

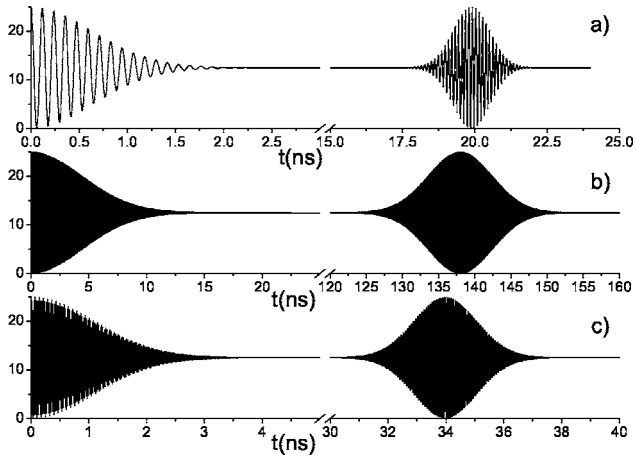

FIG. 6. The average number of photons for three different combinations of the coupling constants k_1, k_2. All parameters are the same as in Fig. 4. The coupling constants and the characteristic time scales are given in Table I.

$$+ \langle \Phi_0|\Big[\frac{1}{2}\sin(\psi_0)^2\sin\Big(\frac{\Omega_R}{2}t\Big)^2(3\tilde{r}(\tilde{r}+1) - (M-\tilde{r})^2 + (\tilde{r}(\tilde{r}+1) - 3(M-\tilde{r})^2)(\cos(2\psi_0) + 2\cos(\Omega_R t)\sin(\psi_0)^2))\Big]|\Phi_0\rangle. \tag{41}$$

Notice that $M\cos(\psi_0)$, $\sin(\psi_0)$, $\tilde{r}$, Ω_R are Casimir operators rather than c numbers; therefore they have to be averaged over the initial state along with the operator of the number of photons (see the example in Appendix C). The equations, Eqs. (40) and (41), are derived in the assumption that the initial state of atoms have zero dipole momentum. But the inversion in the atomic system is allowed to have finite values. Our initial state satisfies these conditions and the comparison of second-order and zeroth-order calculations is provided in Fig. 5 for $Q(t)$. At short time scales the agreement between two approximations is very good.

In a similar way as it was done by Eberly and co-workers [41], we calculate the characteristic times of collapses and revivals in the system by the saddle-point approach. The details are provided in Appendix C. The revival time τ_{rev} is determined by the difference between two adjacent Rabi frequencies Ω_R with $M=n_0$ and $M=n_0+1$. The collapse time τ_{col} has two different asymptotic limits. In the case of very small k_2,

$$\tau_{col}^{(1)} \approx \sqrt{\frac{4(3r-m_0+1)k_1^2+\Delta^2}{k_1^4\sqrt{n_0}}}, \tag{42}$$

and for relatively large nonlinearity but small $1/r$,

$$\tau_{col}^{(2)} = \frac{1}{k_2\sqrt{\sqrt{n_0}r}}. \tag{43}$$

In Fig. 6 we demonstrate a good agreement between these zeroth-order estimates for different ratios k_2/k_1 and the numerical results. It is worth noticing that according to Eq. (43) the collapse time decreases as k_2^{-1}, allowing us to achieve

significant squeezing before the relaxation processes take place.

As we showed the nonlinear term provides additional control on the time scale of quantum effects observed in the system. The quantum squeezing effect is typical for different exactly solvable nonlinear models of quantum optics. As we demonstrate in Appendix A these models are connected with each other in terms of the theory of PAE, and the effective Hamiltonian, Eq. (15), can be well approximated by one of them. The important feature described in our paper is that quantum nonlinearity in the model is controlled by strong classical field A_c.

VI. CONCLUSION

In the paper, we studied different mechanisms of the nonlinear interaction between multiphoton optical pulses and many-particle BECs. The dynamics corresponds to a regime of giant delays in the probe pulse propagation with almost negligible absorption of the pulse in the medium with electromagnetically induced transparency. Using the tree-level Λ scheme within a polarization approach, we find an explicit form of the linear and nonlinear susceptibilities of the atomic condensate characterized with significant transparency induced by the classical field. We studied properties of the condensate refraction index and absorption coefficient related to the probe pulse at frequencies close to the frequency of a corresponding atomic transition. It was demonstrated that the nonlinear refraction index can reach extremely large values. The regions of its negative values and nonlinear dependence of the absorption on the pulse intensity provide a possibility of achieving almost complete compensation of the losses and the dispersion in the BEC.

Applying the formalism of polynomially deformed $su(2)$ algebras, we analyze complex quantum dynamics of the probe pulse in a coherent ensemble of sodium atoms. It was shown that the nonlinear effects provide a necessary window in the relaxation mechanisms, where the probe pulse in the regime of "slow" light exhibits nonclassical properties in statistics of photons. We demonstrated that the Poissonian statistics of photons in the coherent state of the probe pulse can be significantly squeezed within a short period of time to highly sub-Poissonian values due to the collective interaction between coherent atoms and the field. One of the methods to observe reported effects can be based on a typical scheme of balance homodyning in the Mach-Zehnder interferometer with a cell of sodium condensate installed in one of its arms. These results open new perspectives in the generation of nonclassical atomic or field states in a Bose-Einstein condensate controlled by external classical light.

ACKNOWLEDGMENTS

I. V. acknowledges the support of the Engineering and Physical Sciences Research Council. A. P. acknowledges the financial support from the Ministry of Education of Russian Federation through the Grant of President of Russia and RFBR (Russian Foundation for Basic Research) through Grant No. 01-02-17478. A. P. thank G. Leuchs and N. Korolkova for many stimulating discussions.

APPENDIX A: EXACTLY SOLVABLE APPROXIMATIONS OF THE EFFECTIVE MODEL

The method of polynomial algebras of excitations [37] and the quantum inverse scattering method (QISM) [42], as applied to problems in quantum optics, are closely related. Indeed, both methods deal with the algebras of collective excitations in quantum systems. In this appendix we describe better approximations of the effective model, Eq. (15), corresponding to the structure polynomial of the order higher than two. The approximations are exactly solvable in terms of QISM and their connection to the effective model can be established in the framework of the method of PAE. The connection is based on the isomorphism between the PAEs of different orders discussed in our previous work [37].

In the paper we approximated the fifth-order PAE by the $su(2)$ type model, whose structure polynomial is typically of the second order. A next possible exactly solvable approximation is the conventional Tavis-Cummings model corresponding to the third-order PAE (see the third term in Eq. (15)). A better approximation corresponding to the fourth-order PAE is the so-called intensity-dependent models (IDM), whose structure and properties we studied earlier [43]. This family of quantum models is described by the Hamiltonian

$$\mathcal{H} = \tilde{\omega}_0 \tilde{S}_3 + \xi(K_0 - \kappa)\tilde{S}_3 + \tilde{g}(K_+ \tilde{S}_- + K_- \tilde{S}_+). \tag{A1}$$

Here $\tilde{S}_\pm$, $\tilde{S}_3$ are the $su(2)$ operators, while the operators K_0, $K_\pm$ satisfy the $su(1,1)$ algebra $[K_0, K_\pm] = \pm K_\pm$, $[K_-, K_+] = 2K_0$ with $K_-|0;\kappa\rangle = 0$. Different values of the Bargmann index κ deliver different realizations of the $su(1,1)$ algebra in terms of the bosonic Heisenberg-Weyl algebra b, $b^\dagger$. For $\kappa = \frac{1}{2}$, we arrive at the intensity-dependent model through the realization $K_+ = i\sqrt{b^\dagger b}\, b^\dagger$, $K_- = -ib\sqrt{b^\dagger b}$, $K_0 = b^\dagger b + 1/2$. As one may notice, the Hamiltonian, Eq. (A1), is then closely related to the effective model studied in the paper. We define the generators of the fourth-order PAE corresponding to the intensity-dependent model as follows:

$$\Pi_+ = K_+ \cdot \tilde{S}_-, \quad \Pi_- = K_- \cdot \tilde{S}_+,$$

$$\Pi_0 = \frac{K_0 - \tilde{S}_3}{2}, \quad \Pi = (\tilde{S}_3 + \tilde{r}) + (K_0 - \kappa). \tag{A2}$$

Here Π is an analog of the Casimir operator M. The parameters of the structure polynomial read as

$$c_0 = -1, \quad q_1 = \frac{\tilde{r} + k - \Pi}{2}, \quad q_2 = \frac{\tilde{r} + 2 - 3k - \Pi}{2},$$

$$q_3 = \frac{\Pi - 3\tilde{r} + k}{2}, \quad q_4 = \frac{\Pi + \tilde{r} + k + 2}{2}. \tag{A3}$$

It is now straightforward to construct the isomorphism between the algebras of the Hamiltonian, Eq. (15), and Eq.

(A1). Following the steps described in Sec. III, we construct the approximation of the generators $M_{\pm}$ by the generators $\Pi_{\pm}$ and solve the problem.

The solution of a quantum model through the algebraic Bethe ansatz starts with the introduction of the *monodromy* matrix,

$$T(\lambda)=\begin{pmatrix} A(\lambda) & B(\lambda) \\ C(\lambda) & D(\lambda) \end{pmatrix},$$

where $\lambda \in \mathbb{C}$ is a spectral parameter. A fundamental property of the monodromy matrix is that it satisfies the Yang-Baxter equation [42]:

$$R(\lambda-\mu)T(\lambda)\otimes T(\mu)=T(\mu)\otimes T(\lambda)R(\lambda-\mu). \quad \text{(A4)}$$

Here the R matrix $R(\lambda-\mu)$ has the form

$$R(\lambda-\mu)=\begin{pmatrix} f(\mu,\lambda) & 0 & 0 & 0 \\ 0 & g(\mu,\lambda) & 1 & 0 \\ 0 & 1 & g(\mu,\lambda)0 & \\ 0 & 0 & 0 & f(\mu,\lambda) \end{pmatrix}, \quad \text{(A5)}$$

where $f(\mu,\lambda)=1-i/(\lambda-\mu)$, $g(\mu,\lambda)=-i/(\lambda-\mu)$. In the framework of the method of the algebraic Bethe ansatz, the model possesses the vacuum vector $|0\rangle$ such that $A(\lambda)|0\rangle=a(\lambda)|0\rangle$, $D(\lambda)|0\rangle=d(\lambda)|0\rangle$. The eigenvectors of the *transfer* matrix $\tau(\lambda)=A(\lambda)+D(\lambda)$ are constructed through the application of the operators of collective excitations $B(\lambda)$ to the vacuum vector $|0\rangle$, i.e. $\tau(\lambda)B(\lambda_1)\cdots B(\lambda_M)|0\rangle=\theta(\lambda;\{\lambda_i\}_{i=1}^M)\times(\lambda)B(\lambda_1)\cdots B(\lambda_M)|0\rangle$, where $\theta(\lambda;\{\lambda_i\}_{i=1}^M)=a(\lambda)\Pi_{i=1}^M f(\lambda,\lambda_i)+d(\lambda)\Pi_{i=1}^M f(\lambda_i,\lambda)$. The rapidities $\{\lambda_i\}_{i=1}^M$ satisfy the system of Bethe equations,

$$\frac{a(\lambda_n)}{d(\lambda_n)}=\prod_{j=1,j\neq n}^{M}\frac{f(\lambda_j,\lambda_n)}{f(\lambda_n,\lambda_j)}. \quad \text{(A6)}$$

A realization of the formalism described above, which leads to the fourth-order PAE is connected to the monodromy matrix chosen as $T(\lambda)=L_K(\lambda)L_S(\lambda)$. Here

$$L_K(\lambda)=\begin{pmatrix} i\lambda-K_0 & K_+ \\ -K_- & i\lambda+K_0 \end{pmatrix},$$

$$L_S(\lambda)=e^{\phi\sigma_3/2}\begin{pmatrix} i\lambda-\tilde{S}_3 & -\tilde{S}_+ \\ \tilde{S}_- & -i\lambda-\tilde{S}_3 \end{pmatrix}e^{\phi\sigma_3/2}. \quad \text{(A7)}$$

It can be readily seen that the Hamiltonian, Eq. (A1), can be derived as

$$\mathcal{H}=d_1\left.\frac{d\tau(\lambda)}{d\lambda}\right|_{\lambda=0}+\tilde{g}\tau(0)+d_0.$$

Here $\xi=2\tilde{g}\sinh\phi$, $d_1=i\tilde{\omega}_0/2\cosh\phi-i\kappa\tilde{g}\tanh\phi$, $d_0=2(\tanh\phi/\tilde{g}\cosh\phi)(\frac{1}{2}\tilde{\omega}_0-\kappa\tilde{g}\sinh\phi)^2$. The eigenvalues E_M, in accordance with the scheme described above, can be derived as $E_M=d_1(d\theta(\lambda)/d\lambda)|_{\lambda=0}+g\theta(0)+d_0$, while the application of the creation operator of collective excitation $B(\lambda)$ to the vacuum vector $|0\rangle\equiv|0;\kappa\rangle\otimes|-\tilde{r},\tilde{r}\rangle$ creates the eigenstates, whose rapidities satisfy the Bethe equations, Eqs. (A6), with $a(\lambda)=(i\lambda+\tilde{r})(i\lambda-\kappa)$, $d(\lambda)=-(i\lambda-\tilde{r})(i\lambda+\kappa)$. The operator $B(\lambda)$ has the form $B(\lambda)=(i\lambda-\tilde{S}_3)K_+-\tilde{S}_+(i\lambda+K_0)$. This concludes the exact solution of the intensity-dependent Tavis-Cummings model. In the end it is worth mentioning that the intensity-dependent Tavis-Cummings model is advantageous because it exhibits very strong squeezing properties [44].

APPENDIX B: UNITARY TRANSFORMATIONS

After the transformation $U_0=e^{i\psi_0\tilde{S}_y}$, the Hamiltonian Eq. (33) reads as

$$U_0H^{(2)}U_0^{-1}=C_0+\Omega_R\tilde{S}_3-k\frac{\beta_1}{4}[\cos(2\psi_0)(\tilde{S}_3\tilde{S}_x+\tilde{S}_x\tilde{S}_3)+\sin(2\psi_0)(\tilde{S}_3^2-\tilde{S}_x^2)]$$
$$-k\frac{\beta_2}{2}\left[\begin{array}{c}(\cos(3\psi_0)+\cos(\psi_0)\sin(\psi_0)^2)\tilde{S}_3\tilde{S}_x\tilde{S}_3-(\sin(3\psi_0)-\sin(\psi_0)\cos(\psi_0)^2)\tilde{S}_x\tilde{S}_3\tilde{S}_x \\ +\sin(\psi_0)\tilde{S}_3\left(\cos(\psi_0)^2(\tilde{S}_3^2-1)+\frac{1}{4}\right)+\cos(\psi_0)\tilde{S}_x\left(\sin(\psi_0)^2(\tilde{S}_x^2-1)+\frac{1}{4}\right)\end{array}\right]. \quad \text{(B1)}$$

To diagonalize the operator, Eq. (B1), in first order of $\beta_1\sim\alpha$, we apply second unitary transformation,

$$U_1=\exp\left[-i\frac{\beta_1}{4}\sin(\psi_0)\left((\tilde{S}_3\tilde{S}_y+\tilde{S}_y\tilde{S}_3)\cos(2\psi_0)\right.\right.$$
$$\left.\left.-\frac{1}{4}(\tilde{S}_x\tilde{S}_y+\tilde{S}_y\tilde{S}_x)\sin(2\psi_0)\right)\right]. \quad \text{(B2)}$$

It is obvious that the transformation U_1 applied to the zeroth order term in Eq. (B1) produces the first-order term in the original Hamiltonian, however with an opposite. Therefore these terms are mutually cancelled. Thus, the Hamiltonian $U_1U_0H^{(2)}U_0^{-1}U_1^{-1}$ is diagonal up to second order of α. It has the form

$$U_1U_0H^{(2)}U_0^{-1}U_1^{-1} = C_0 + \Omega_R\tilde{S}_3 - k\frac{\beta_1}{4}\sin(\psi_0)\cos(\psi_0)(3\tilde{S}_3^2 - \tilde{r}(\tilde{r}+1)) + k\left(\frac{\beta_1}{4}\right)^2\sin(\psi_0)$$
$$\times\left[\begin{array}{c}\cos(2\psi_0)^2\tilde{S}_3\left(4\tilde{S}_3^2 - 2\tilde{r}(\tilde{r}+1) + \frac{1}{2}\right) + \frac{\sin(2\psi_0)^2}{4}\tilde{S}_3\left(5\tilde{S}_3^2 - 5\tilde{r}(\tilde{r}+1) + \frac{11}{2}\right)\\ + 3\sin(2\psi_0)^2\tilde{S}_x\tilde{S}_3\tilde{S}_x - \frac{\sin(4\psi_0)}{2}\left(9\tilde{S}_3\tilde{S}_x\tilde{S}_3 + \tilde{S}_x^3 - \frac{6\tilde{r}(\tilde{r}+1)-13}{4}\tilde{S}_x\right)\end{array}\right]$$
$$-k\frac{\beta_2}{2}\left[\begin{array}{c}(\cos(3\psi_0)+\cos(\psi_0)\sin(\psi_0)^2)\tilde{S}_3\tilde{S}_x\tilde{S}_3 - (\sin(3\psi_0)-\sin(\psi_0)\cos(\psi_0)^2)\tilde{S}_x\tilde{S}_3\tilde{S}_x\\ + \sin(\psi_0)\tilde{S}_3\left(\cos(\psi_0)^2(\tilde{S}_3^2-1)+\frac{1}{4}\right) + \cos(\psi_0)\tilde{S}_x\left(\sin(\psi_0)^2(\tilde{S}_x^2-1)+\frac{1}{4}\right)\end{array}\right]. \quad \text{(B3)}$$

Notice that we only keep terms of order α or α^2. Therefore, the last term in Eq. (B1) stays intact after the transformation. One can see that the first-order correction vanishes in the case of exact resonance $\Delta=0$. So, it is necessary to consider second-order terms to take into account significant effects connected with the nonlinear dependence of the energy splitting on the value of collective atom-field quasispin vector $\tilde{S}_3$.

To diagonalize the operator Eq. (B3) up to the order α^2, we apply the third unitary transformation,

$$U_2 = \exp\left[\begin{array}{c}i\left(\frac{\beta_1}{4}\sin(\psi_0)\right)^2\left\{\frac{3}{4}\sin(\psi_0)^2(\tilde{S}_x\tilde{S}_3\tilde{S}_y + \tilde{S}_y\tilde{S}_3\tilde{S}_x) + \frac{\sin(4\psi_0)}{2}\left(\frac{1}{3}\tilde{S}_y^3 - 8\tilde{S}_3\tilde{S}_y\tilde{S}_3 + \frac{\tilde{r}(\tilde{r}+1)}{2}\tilde{S}_y - \frac{31}{12}\tilde{S}_y\right)\right\}\\ -i\frac{\beta_2}{2}\sin(\psi_0)\left\{\begin{array}{c}2\cos(3\psi_0)\tilde{S}_3\tilde{S}_y\tilde{S}_3 + \frac{1}{2}\cos(\psi_0)\tilde{S}_y + \frac{1}{2}\sin(\psi_0)\cos(\psi_0)^2(\tilde{S}_y\tilde{S}_3\tilde{S}_x + \tilde{S}_x\tilde{S}_3\tilde{S}_y)\\ -\frac{\sin(3\psi_0)}{2}(\tilde{S}_y\tilde{S}_3\tilde{S}_x + \tilde{S}_x\tilde{S}_3\tilde{S}_y) - \cos(\psi_0)\sin(\psi_0)^2\tilde{S}_y\left(\frac{2}{3}\tilde{S}_y^2 - 2\tilde{r}(\tilde{r}+1) + \frac{10}{3}\right)\end{array}\right\}\end{array}\right]. \quad \text{(B4)}$$

Consecutively applying these three transformations $U_{0,1,2}$ to the Hamiltonian, Eq. (33), we obtain the diagonal operator, Eq. (35).

APPENDIX C: THE COLLAPSE AND REVIVAL CHARACTERISTIC TIMES

According to the zeroth-order solution, Eq. (40), a dynamics of the average number of photons for the initial state, Eq. (39), has the form

$$\bar{n}(t) = \sum_{n=0}^{\infty}\frac{nn_0^n e^{-n_0}}{n!}\frac{k_n^2 + 2\Delta^2 + k_n^2\cos(\sqrt{k_n^2+\Delta^2}t)}{2(k_n^2+\Delta^2)}, \quad \text{(C1)}$$

where, based on Eqs. (30) and (31), we defined

$$k_n = \left(k_1 + k_2\frac{n+1}{2}\right)\sqrt{2(4r-n+1)}. \quad \text{(C2)}$$

Deriving the expressions, we used the fact that our initial state belongs to the nearby zones ($\tilde{r}=M/2$), and the atoms are completely unexcited ($M=n, m_0=-r$). For simplicity of the analytical expressions below, we represent the results only for $m_0=-r$. However, these results can be easily generalized to an arbitrary initial number of excitations in an atomic subsystem. Since we are interested in the time dependence of $\bar{n}(t)$, the constant terms in Eq. (C1) can be omitted. We estimate the sum of the time-dependent term using the saddle-point method, which has been applied to calculate the one-atom model [41]. Denoting the time-dependent term in Eq. (C1) by $w(t)$, we can write

$$w(t) \approx \int_0^{\infty}\sqrt{\frac{n}{2\pi}}\frac{k_n^2}{2(k_n^2+\Delta^2)}\,\mathrm{Re}(e^{-n_0+n_0f(n/n_0)})dn, \quad \text{(C3)}$$

where

$$f(x) = x(1-\ln x) + it\sqrt{\frac{\Delta^2}{n_0^2} + \left(2r+\frac{1}{2}-\frac{n_0x}{2}\right)\left(\frac{2k_1+k_2}{n_0}+k_2x\right)^2}. \quad \text{(C4)}$$

We find

$$w(t) \approx \frac{n_0k_{n_0}^2}{2(k_{n_0}^2+\Delta^2)}\,\mathrm{Re}\left(\frac{e^{-n_0+n_0f(x_0)}}{\sqrt{f''(x_0)}}\right), \quad \text{(C5)}$$

where the point x_0 is the saddle point of the analytical function $f(x)$, i.e., $f'(x_0)=0$. It follows from the definition that the saddle-point x_0 depends on the time. As it was explained in

TABLE I. Characteristic time scales for three different combinations of the coupling constants in sodium BEC.

	k_1/ω	k_2/ω	T_R (ns)	$\tau_{col}^{(1)}$ (ns)	$\tau_{col}^{(2)}$ (ns)	τ_{rev} (ns)
a)	3E−7	−3E−9	0.12	41.1.	2.1	19.9
b)	3E−7	−3E−10	0.10	41.1	20.8	138
c)	3E−6	−3E−10	0.01	4.1	20.8	34

detail in the paper [41], the collapse time τ_{col} is roughly estimated by the condition

$$|1 - \mathrm{Re}\, f(x_0)| = \sqrt{n_0}. \tag{C6}$$

For the moment τ_{col} when the condition Eq. (C6) is fulfilled, the exponent in Eq. (C5) becomes very small and the envelope of the sinusoidal oscillations "collapses." For $t=0$ it is plain to see that $x_0=1$.

Expanding the solution for x_0 in the vicinity of unity and substituting it into Eq. (C6), we obtain a relatively lengthy expression. If we assume that the nonlinear susceptibility k_2 is the dominating smallness parameter, and expand the result with respect to $k_2 \to 0$, we find

$$\tau_{col}^{(1)} \approx \sqrt{\frac{4(3r - m_0 + 1)k_1^2 + \Delta^2}{k_1^4\sqrt{n_0}} + 4k_2\frac{k_1^2(8r - n_0 + 1)(4r + 1) - (2r - n_0)\Delta^2}{k_1^5\sqrt{n_0}}}. \tag{C7}$$

Assuming that the leading smallness parameter is $1/r$, we obtain an expression for relatively large nonlinearity k_2,

$$\tau_{col}^{(2)} = \frac{1}{k_2\sqrt{\sqrt{n_0}r}}\sqrt{1 + \frac{8k_1^4 + 6k_1^2k_2^2(2n_0 + 1) + 4k_1^3k_2(2n_0 + 3) + k_1k_2^3\left(\frac{\Delta^2}{k_2^2} + 6n_0 + 1\right) + k_2^4\left(n_0 - \frac{\Delta^2}{k_2^2}\left(n_0 - \frac{1}{2}\right)\right)}{2rk_2(2k_1 + k_2)^3}}. \tag{C8}$$

Even for $k_2=0$ in Eq. (C7), our results cannot be directly compared with Eberly's paper because we consider the dynamics in the nearby zones, which do not exist in the simple one-atom model. However, it is not difficult to obtain corresponding results for the remote zones, which are more relevant to their work. We also want to notice that the solutions Eqs. (C7) and (C8), provide additional information about the dependence of collapse times on the number of particles in BEC, which is completely opposite in these two asymptotical limits.

The revival time is estimated by the period when the phases of oscillations of neighboring terms in Eq. (C1) with frequencies k_n differ by 2π. The difference is estimated for the dominant sinusoids with $n=n_0$ and $n=n_0+1$. The revival time reads as

$$\tau_{rev} \approx \left|\frac{2\pi}{\sqrt{k_{n_0+1}^2 + \Delta^2} - \sqrt{k_{n_0}^2 + \Delta^2}}\right|. \tag{C9}$$

The Rabi oscillation period T_R in Table I is estimated as

$$T_R \approx \frac{2\pi}{\sqrt{k_{n_0}^2 + \Delta^2}}. \tag{C10}$$

[1] M. O. Scully and M. S. Zubairy, *Quantum Optics* (Cambridge University Press, Cambridge, England, 1997).

[2] E. Wolf, in *Progress In Optics* (Elsevier Science B. V., Netherlands, Amsterdam, 2000), Vol. 43, p. 512 (2002).

[3] A. Imamoglu, H. Schmidt, G. Woods, and M. Deutsch, Phys. Rev. Lett. **79**, 1467 (1997).

[4] H. Wang, D. Goorskey, and M. Xiao, Opt. Lett. **27**, 258 (2002).

[5] N. G. Basov, R.V. Abartsumian, V. S. Zuev, P. G. Kryukov, and V. S. Letokhov, Sov. Phys. JETP **23**, 16 (1966).

[6] N. G.Basov and V. S. Letokhov, Sov. Phys. Dokl. **11**, 222 (1966).

[7] C. G. B. Garrett and D. E. McCumber, Phys. Rev. A **1**, 305 (1970).

[8] S. Chu and S. Wong, Phys. Rev. Lett. **48**, 738 (1982).

[9] L. Allen and J. Ebebley, *Optical Resonance and Two-Level Atoms* (Mir, Moscow, 1978).

[10] S. E. Harris, J. E. Field, and A. Imamoglu, Phys. Rev. Lett. **64**, 1107 (1990).

[11] G. Alzetta, A. Gozzini, L. Moi, and G. Orriols, Nuovo Cimento Soc. Ital. Fis., B **36**, 5 (1976).

[12] H. R. Gray, R. M. Whitley, and C. R. Stroud, Opt. Lett. **3**, 218 (1978).

[13] S. P. Tewari and G. S. Agarwal, Phys. Rev. Lett. **56**, 1811 (1986).

[14] S. E. Harris, J. E. Field, and A. Kasapi, Phys. Rev. A **46**, R29 (1992).

[15] A. V. Turukhin, V. S. Sudarshanam, M. S. Shahriar, J. A. Musser, B. S. Ham, and P. R. Hemmer, Phys. Rev. Lett. **88**, 023602 (2002).

[16] M. D. Lukin, P. R. Hemmer, M. Loffler, and M. O. Scully, Phys. Rev. Lett. **81**, 2675 (1998).

[17] H. Wang, D. Goorskey, and M. Xiao, Phys. Rev. Lett. **87**, 073601 (2001).

[18] W. Ketterle, Rev. Mod. Phys. **74**, 1131 (2002).

[19] E. A. Cornell and C. E. Wieman, Rev. Mod. Phys. **74**, 875 (2002).

[20] L. N. Hau, S. E. Harris, Z. Dutton, and C. H. Behroozi, Nature (London) **397**, 594 (1999).

[21] J. J. McClelland and M. H. Kelley, Phys. Rev. A **31**, 3704

(1985).
[22] M. Mitsunaga, M. Yamashita, and H. Inoue, Phys. Rev. A **62**, 013817 (2000).
[23] M. Leontovich, Izv. Akad. Nauk SSSR, Ser. Fiz **8**, 16 (1944).
[24] A. K. Patnaik, J. Q. Liang, and K. Hakuta, Phys. Rev. A **66**, 063808 (2002).
[25] Y. R. Shen, *The Principles of Nonlinear Optics*, edited by John Wiley and Sons (University of California, Berkeley, 1984).
[26] M. D. Lukin and A. Imamoglu, Phys. Rev. Lett. **84**, 1419 (2000).
[27] D. N. Kli'shko, *Physical Foundations For Quantum Electronics* (Moscow, Nauka, 1986).
[28] A. V. Prokhorov, A. P. Alodjants, and S. M. Arakelian, JETP Lett. **80**, 739 (2004).
[29] G. P. Agrawal, *Nonlinear Fiber Optics*, (Academic, San Diego, 2001).
[30] S. Al-Awfi and M. Babiker, Phys. Rev. A **58**, 4768 (2000).
[31] S. E. Harris and L. V. Hau, Phys. Rev. Lett. **82**, 4611 (1999).
[32] M. Mitchell and R. Chiao, Phys. Lett. A **230**, 133 (1997).
[33] M. Tavis and F. Cummings, Phys. Rev. **170**, 379 (1968).
[34] R. Dicke, Phys. Rev. **93**, 99 (1954).
[35] A. Andre and M. D. Lukin, Phys. Rev. Lett. **89**, 143602 (2002).
[36] A. Icsevgi and W. E. Lamb, Phys. Rev. **185**, 517 (1954).
[37] I. P. Vadeiko, G. P. Miroshnichenko, A. V. Rybin, and J. Timonen, Phys. Rev. A **67**, 053808 (2003).
[38] S. M. Chumakov, A. B. Klimov, and J. J. Sanchez-Mondragon, Phys. Rev. A **49**, 4972 (1994).
[39] C. Saavedra, A. B. Klimov, S. M. Chumakov, and J. C. Retamal, Phys. Rev. A **58**, 4078 (1998).
[40] J. Delgado, E. C. Yustas, L. L. Sanchez-Soto, and A. B. Klimov, Phys. Rev. A **63**, 063801 (2001).
[41] J. H. Eberly, N. B. Narozhny, and J. J. Sanchez-Mondragon, Phys. Rev. Lett. **44**, 1323 (1980).
[42] V. Korepin, N. Bogoliubov, and A. Izergin, *Quantum Inverse Scattering Method and Correlation Functions* (Cambridge University Press, Cambridge, 1994).
[43] I. Vadeiko, "Dynamics and collective effects in cavity QED and in Bose-Einstein condensation," Ph.D. thesis, University of Jyvaskyla, Finland. ISBN 951-39-1322-8, ISSN 0075-465X, 2002.
[44] A. Rybin, G. Miroshnichenko, I. Vadeiko, and J. Timonen, J. Phys. A **32**, 8739 (1999).